Published in final edited form as:
J Control Release. 2011 September 5; 154(2): 171–176. doi:10.1016/j.jconrel.2011.06.016.

Poly(β-amino ester) - DNA complexes: time-resolved fluorescence and cellular transfection studies

Elina Vuorimaa[a], **Tiia-Maaria Ketola**[a], **Jordan J. Green**[b], **Martina Hanzlíková**[c], **Helge Lemmetyinen**[a], **Robert Langer**[d], **Daniel G. Anderson**[d], **Arto Urtti**[e], and **Marjo Yliperttula**[c,*]

[a]Department of Chemistry and Bioengineering, Tampere University of Technology, P.O. Box 541, FIN-33101 Tampere, Finland [b]Biomedical Engineering and the Institute for Nanobiotechnology, The Johns Hopkins University School of Medicine, 400 N Broadway, Smith Building 5017, Baltimore, MD 21231, USA [c]Division of Biopharmaceutics and Pharmacokinetics, Faculty of Pharmacy, P. O. Box 56, FI-00014 University of Helsinki, Finland [d]The David H. Koch Institute for Integrative Cancer Research, Massachusetts Institute of Technology, 77 Massachusetts Avenue , Cambridge, MA 02139, USA [e]Centre for Drug Research, Faculty of Pharmacy, P. O. Box 56, FI-00014 University of Helsinki, Finland

Abstract

A large number of different polymers have been developed and studied for application as DNA carriers for non-viral gene delivery, but the DNA binding properties are not understood. This study describes the efficiency of nanoparticle formation by time-resolved fluorescence measurements for poly(β-amino esters), cationic biodegradable polymers with DNA complexation and transfection capability. From the large library of poly(β-amino esters) ten polymers with different transfection efficacies were chosen for this study. The binding constants for nanoparticle formation were determined and compared to polyethylene imines with the same method. Although the DNA binding efficiency of the amine groups are similar for both types of polymers, the overall binding constants are an order of magnitude smaller for poly(β-amino esters) than for 25 kDa polyethylenimines, but yet poly(β-amino esters) show comparable DNA transfection efficacy with polyethyleneimines. Within this series of polymers the transfection efficacy showed increasing trend in association with relative efficiency of nanoparticle formation.

Keywords

gene delivery; poly(β-amino esters); DNA complexation; DNA binding; time-resolved fluorescence spectroscopy

1. Introduction

The viruses are able to transfer their genetic cargo to the host cells. Although most of current gene therapy research relies on viral vectors, safety problems (incl. deaths in clinical trials)

* Corresponding author: Marjo Yliperttula, Division of Biopharmaceutics and Pharmacokinetics, Faculty of Pharmacy, P. O. Box 56, FI-00014 University of Helsinki, Finland, tel: +358-9-440935566, fax: +358-9-191 59580, marjo.yliperttula@helsinki.fi.

have slowed down the progress of this approach [1-3]. Non-viral (chemical) vectors, based on nanoparticles, are potential alternatives to the viral vectors. They offer advantages that are difficult to achieve with viral vectors: versatility, lack of immunogenicity, easy large-scale production, unrestricted DNA size, and possibility to incorporate several different DNA species to the same particle [4]. However, the chemical vectors show poor transfection efficacy [5]. Typical non-viral DNA delivery systems involve polycationic species, like cationic polymers, cationic liposomes or micelles, that complex and condense plasmid DNA in solution forming nanoparticles of 40–500 nm in diameter [6-9]. Nanoparticle mediated gene transfection involves several phases: DNA complexation, binding to the cell surface, endocytic uptake, endosomal escape to the cytosol, nuclear entry, transcription and translation. Importantly, DNA must be released from the nanoparticles before transcription.

Poly(β-amino esters) (PBAEs) [10-13] are promising agents for non-viral gene delivery due to their (1) large potential for structural diversity, (2) ability to condense DNA into small and stable nanoparticles, (3) ability to buffer the endosome and facilitate endosomal escape, (4) biodegradability via hydrolytic cleavage of ester groups, (5) low cytotoxicity compared with some other cationic polymers, and (6) relatively high efficacy *in vitro* and *in vivo*. The best PBAEs are linear, synthesized at an amine/acrylate ratio of 1.2:1, and have a molecular weight of ~10 kDa [13,14].

Steady state fluorescence measurements of ethidium bromide are widely used to characterize DNA binding by cationic polymers and lipids. Due to the overlapping and broad spectra of free and DNA bound ethidium bromide, this method cannot be used in quantitative manner to resolve the binding constants of DNA and cationic polymers. Previously [15] we demonstrated that the nanoparticle formation and DNA-polymer binding constants and possible multiple states of binding can be determined with time-resolved fluorescence using ethidium bromide (ETI) as the fluorescent probe. Because fluorescence lifetimes and their proportions instead of intensity are used to analyze the state of the system, the method is not hampered by scattering and thus allowing more quantitative analysis than steady state measurements. The method revealed DNA complexation differences between an efficient transfection agent (polyethylenimine; PEI) and poor transfection agent (poly-L-lysine; PLL). For these polymers both the nature and the density of the amine groups taking part in the complexation of DNA are different: PEI contains primary, seconday and tertiary amines, whereas PLL includes only primary amines.

The purpose of this study was to extend the detailed DNA binding constant analyses to polymers with only tertiary amines. From a large library of PBAEs [13] ten polymers with different transfection efficacies were chosen for this purpose. We determined the DNA–complexation behaviour of different PBAEs over a wide amine to phosphate (N/P) range, from 1 to 100, to reveal the complexation efficiency and mechanism, and to determine the binding constants for the studied PBAEs. In addition, we investigated a possible correlation between fluorescence parameters and transfection efficacy of PBAEs.

2. Materials and methods

2.1. Materials

Plasmid DNA (pCMVβ) that encodes β-galactosidase reporter gene was produced in *E. coli*, and isolated and purified using a Qiagen Plasmid Giga kit (Qiagen, Germany). Ten different poly(β-amino esters) (PBAEs) (Table 1) with average molecular weights ranging from 8 to 28 kDa were synthesized by the conjugate addition of amine monomers (numbers) to diacrylate monomers (letters) solvent free at 95°C or in DMSO at 60°C [12]. The reaction proceeds in one step without the production of any byproducts. The PBAEs were then

dissolved in DMSO to 100 mg ml^{-1} concentration and were further diluted into 50 mM MES-HEPES buffer (pH 7.4) to a final concentration of 6 mg ml^{-1}.

2.2. Sample preparation

All solutions were prepared in 50 mM MES-HEPES buffer (pH 7.4). In preparing the Polymer/DNA complexes, the molar ratio of PEI nitrogen to DNA phosphate (N/P ratio) was used. The final DNA concentration was adjusted to 0.0975 mg ml^{-1}, i.e. 300 μM per nucleotide and the ethidium bromide (ETI) : nucleotide ratio was 1:15. With the DNA:ETI molar ratio used ETI is fully bound by DNA, which is observed as one-exponential decay in the presence of DNA. The polyplexes were prepared by mixing the (DNA) : (ETI) solution and the cationic polymer solution at volume ratio of 1:1. Solutions were mixed rigorously to ensure effective complexation between DNA and the polymer.

2.3. Fluorescence measurements

The time-resolved fluorescence was measured using a time-correlated single photon counting (TCSPC) system (PicoQuant GmBH) consisting of PicoHarp 300 controller and PDL 800-B driver. The samples were excited with the pulsed diode laser head LDH-P-C-485 at 483 nm and the time resolution was about 130 ps. The signals were detected with a microchannel plate photomultiplier tube (Hamamatsu R2809U). To diminish the influence of the scattered excitation, a cutoff filter was used in front of the monitoring monochromator. To study the time-resolved spectra the decays were collected with a constant accumulation time (300 s) in the 560– 670 nm wavelength range with steps of 10 nm. The decays were simultaneously fitted to the sum of exponents in the equation $I(t,\lambda) = \sum a_i(\lambda)\, e^{-t/\tau_i}$, where τ_i is the global the lifetime and $a_i(\lambda)$ is the local the pre-exponential factor at a particular wavelength. The factors $a_i(\lambda)$ represent the decay-associated spectra (DAS), which in the case of a mixture of different non-interacting fluorescing species correspond to the individual spectra of the species. The amplitudes were corrected according to the sensitivity of the detector at different wavelengths and the relative fluorescence quantum yields of the components. The relative fluorescence quantum yield of free ETI $\Phi_{ETI}^{rel} = 0.273$ when $\Phi_{ETI:DNA}^{rel}$ for the ETI:DNA complex is set to 1. The spectral areas (A_i) of the components were calculated by integrating the corrected pre-exponential factors over the measured wavelength range. The proportions of the decay components can be calculated from the spectral areas of the components as $x_2 = [A_i/(A_1 + A_2)] \times 100\%$

3. Results

The degree of DNA condensation was determined as a function of the polymer/DNA N/P ratio by a time-resolved fluorescence method using ethidium bromide (ETI). ETI shows significant enhancement of fluorescence intensity and lifetime upon intercalation with DNA (23 ns) compared to that in bulk buffer (1.9 ns) [16-18]. During the nanoparticle formation the ETI molecules intercalated in the DNA double helix are displaced by interaction with polycations and ETI is freed into the bulk solution. The two lifetime values are so distinct that their relative contribution can be used to estimate the extent of nanoparticle formation [15,19].

The fluorescence decays in the presence of all the PBAEs studied here are clearly two exponential. As an example, the decays observed at 610 nm for C32 at different N/P ratios are shown in Fig. 1. The fluorescence lifetimes stay constant irrespective of the N/P ratio and the average lifetimes for each polymer are listed in Table 2.

The lifetimes of the long-living component obtained in the presence of PBAEs are similar to the values obtained for ETI:DNA complex in the absence of PBAEs. The lifetimes of the short-living component are nearly equal to free ETI in the absence of DNA. The proportion of the short-living decay component, x_1, increases with increasing N/P ratio for all polymers (Fig. 2). Very small differences between the polymers are observed although for C36 and F28 the increase is less than for the others. The increase in the proportion of the short-living component is also clearly observed in Fig. 3, where the decay associated spectra for C36 and C28 at N/P ratios 25 and 100 are presented. The shape of the shorter-living component resembles closely to that of free ETI for all cases. The shape of the longer-living component is broader than for ETI:DNA complex in the absence of the polymers and the maximum is red shifted from 600 to 610 nm. These changes are usually observed during nanoparticle formation: the proportion of free ETI in the system corresponds to the formation of tightly bound polymer:DNA complexes and the changes observed in the longer-living component correspond to the changes in the environment of the DNA that is not yet tightly bound by the polymer [18].

Binding constants

In a previous study [15,18] on the polyplex formation between polyethylenimine (PEI) and DNA, we used the time-resolved fluorescence data to determine the binding constants. To compare the behavior of the present PBAEs with PEIs, the binding constants for PBAEs were determined in the same way. The corrected spectral areas A_1^c obtained for the short-living component correspond to the amount of polyplex and the values A_2^c obtained for the long-living component correspond to the amount of unbound DNA. The ratio A_2^c/A_1^c can be expressed as [18]:

$$\frac{A_2^c}{A_1^c} = C + \frac{1}{K[P]} \quad (1)$$

where K is the binding constant of the overall equilibrium, [P] is the concentration of the polymer and C is a proportionality factor correcting the difference between the spectroscopic data and the actual concentration. Plotting the ratio A_2^c/A_1^c as a function of the inverse PBAE concentration (as mol N-groups dm^{-3}) a linear dependence was observed for all PBAEs at least up to N/P ratio 50. At this N/P ratio, the complexation seems to have reached equilibrium and the A_2^c/A_1^c ratio remained nearly constant with increasing [P]. For some polymers, further decrease in the A_2^c/A_1^c ratio was observed (Fig. 4) indicating that the formed polyplexes start to aggregate at higher N/P ratios. Examples of both types of behavior are shown in Fig. 6. The binding constants per N-group calculated from the slopes were between 2000 and 6300 $dm^3\ mol^{-1}$ N-groups for all PBAEs (Table 3). These values are similar to those obtained for PEIs (2100–6600 $dm^3\ mol^{-1}$ N-groups).

Efficiency of nanoparticle formation

The spectral areas of each component, A_i, represent the amount of the component in the system. The differences of the spectral areas of the components in the decay associated spectra (Fig. 3) are however relatively small and thus prone to experimental errors. To obtain more reliable tool for estimating the relative efficiency of polyplex formation by the studied PBAEs, the maximum amplitudes $a_{i,max}$ at each N/P ratio were used. The relative efficiency was estimated as the difference in the ratio of the maximum amplitudes of the two fluorescence components $a_{i,max}$ at each N/P ratio according to equation 3:

$$\text{Relative efficiency} = \frac{\left(\frac{a_{1,max}}{a_{2,max}}\right)_{N/P} - R_{min}}{R_{max} - R_{min}} \quad (2)$$

where $R_{max} = \left[\left(\frac{a_{1,max}}{a_{2,max}}\right)_{100}\right]_{max}$ is the maximum amplitude ratio at N/P =100 and $R_{min} = \left[\left(\frac{a_{1,max}}{a_{2,max}}\right)_{1}\right]_{min}$ is the minimum amplitude ratio at N/P = 1 obtained for this series of polymers. The relative nanoparticle formation efficiency was considered to be 0 % at N/P ratio 1 at which there is minimal interaction between polymer and DNA. For 100 % relative nanoparticle formation efficiency N/P ratio 100 was used, since at this N/P no further changes in the fluorescence signal was observed and it is clearly higher than the useful N/P ratio for transfection (about 50 [14]). Thus, we calculated the nanoparticle formation efficiency for this N/P ratio 50. The obtained relative efficiencies are presented in Fig. 5, and they are compared in Fig. 6 with the relative transfection efficacy of the polymers that was reported earlier [14]. The increased relative nanoparticle formation efficiency is positively correlated with the increased transfection efficacy for most of the polymers.

4. Discussion

Previously we demonstrated differences between DNA nanoparticle formation with PEI and PLL. In general PEI shows higher transfection activity than PLL. Unlike PLL, that has only primary amines, the branched PEI includes primary, secondary and tertiary and high charge density. PEI has a high density of groups with pK_a values close to 7. These groups are able to buffer the acidic environment of the endosome and facilitate endosomal escape through the “proton sponge” mechanism [20-22]. According to our previous studies both branched and linear 22 kDa PEI condense DNA into nanoparticles via a two step equilibrium: first of loosely bound DNA:PEI intermediate complex is formed followed by the formation of the tightly bound DNA:PEI nanoparticle. The rate of formation for the tightly bound nanoparticle is much higher than for the loosely bound complex. Thus, the amount of the loosely bound complex remains very small during the polyplex formation. This deviates from the single step nanoparticle formation with PLL.

In this study, we investigated DNA complex formation with PBAEs that have previously shown to have good transfection activity. Like in the case of PEI, the tertiary amines of PBAEs are able to buffer the endosomes and facilitate cytoplasmic delivery of DNA. However, the PBAE mediated DNA complexation took place in one step. Although the binding constants per nitrogen atom are similar in PBAEs and PEI, the binding constants per polymer molecule are 2 -68 times smaller lower for PBAEs than for high molecular weight PEIs. This is due to the structure of the PBAEs: the density of N-groups in the polymer chain is much lower than for PEIs. The distance between the N-groups is so long that the co-operativity of binding to DNA is lower than for PEIs. The PBAEs also have lower ratio of primary and secondary amines to tertiary amines compared to PEI. As a consequence, the PBAEs require more N-groups than PEI in order to fully complex DNA. Typically, high N/P ratios of about 50:1 are needed for efficient transfection compared with about 6:1 as used for high molecular weight PEIs [13]. To further modify the function of PBAEs, the end groups of the diacrylate-terminated polymers have been substituted with primary amines [24-26]. This increases the cationic charge of the polymers, improves DNA binding affinity and condensation of DNA into nanoparticles. Such derivative (C32) was highly effective in transfection [24]. In fact, PBAE polymer mediated transfection seems to improve with increasing nanoparticle formation. This may be related to the overall weak DNA binding

levels. On the contrary, for tight DNA binders further increase in binding affinity is expected to decrease transfection due to the impaired DNA release in the cells.

One of the crucial steps for efficient gene delivery is the release of DNA from the nanoparticle to the cytosol. Because this process is the reverse reaction of the nanoparticle formation, for PEIs this takes place in two steps. The present results suggest that with PBAEs, this process takes place in one step, but the low DNA binding constants of PBAEs are expected to facilitate DNA release. This process involves exchange reaction in which polycation will bind to the cellular polyanions thereby rendering pDNA free [23]. On longer time scales the degradation of PBAEs in the cells may provide another mechanism for DNA release.

DNA binding affinity and nanoparticle formation efficiency are important parameters for effective non-viral polymeric gene delivery and these parameters can be designed by tuning polymer structure.

5. Conclusions

Recently introduced time-resolved fluorescence assay was applied to estimate the relative efficiency of DNA complexation by poly(β-amino ester)s. The binding constants per amine were in the same order of magnitude for PBAEs and branched 25 kDa PEI, but the overall binding constants per PBAE molecule were ~10 times smaller. This explains why the N/P ratios needed for the formation of DNA:PBAE nanoparticles are ~10 times higher. In contrast with PEI, PBAEs complex DNA in one step, but still they are able to release DNA effectively.

Acknowledgments

This work was supported by the Academy of Finland and by NIH grants CA132091 and CA115527.

References

1. Thomas CE, Ehrhardt A, Kay MA. Progress and problems with the use of viral vectors for gene therapy. Nature Reviews Genetics. 2003; 4:346–358.
2. Check E. Gene therapy put on hold as third child develops cancer. Nature. 2005; 433:561.
3. Nayak S, Herzog RW. Progress and prospects: immune responses to viral vectors. Gene Ther. 2010; 17:295–304. [PubMed: 19907498]
4. Li S, Huang L. Non-viral is superior to viral gene delivery. J Control Rel. 2007; 123:181–183.
5. Pack DW, Hoffman AS, Pun S, Stayton PS. Design and development of polymers for gene delivery. Nat Rev Drug Discov. 2005; 4:581–593. [PubMed: 16052241]
6. Boussif O, LezoualC'H F, Zanta MA, Mergny MD, Scherman D, Demeneix B, et al. A versatile vector for gene and oligonucleotide transfer into cells in culture and in vivo: Polyethylenimine. Proc Natl Acad Sci USA. 1995; 92:7297–7301. [PubMed: 7638184]
7. Mahato RI. Water insoluble and soluble lipids for gene delivery. Adv Drug Deliv Rev. 2005; 57:699–712. [PubMed: 15757756]
8. Pelisek J, Gaedtke L, DeRouchey J, Walker GF, Nikol S, Wagner E. Optimized lipopolyplex formulations for gene transfer to human colon carcinoma cells under in vitro conditions. J Gene Med. 2006; 8:186–197. [PubMed: 16245365]
9. Merdan T, Kopeček J, Kissel T. Prospects for cationic polymers in gene and oligonucleotide therapy against cancer. Adv Drug Deliv Rev. 2002; 54:715–758. [PubMed: 12204600]
10. Lynn DM, Langer R. Degradable poly(b-amino esters): Synthesis, characterization, and self-assembly with plasmid DNA. J Am Chem Soc. 2000; 122:10761–10768.

11. Lynn DM, Anderson DG, Putnam D, Langer R. Accelerated discovery of synthetic transfection vectors: Parallel synthesis and screening of a degradable polymer library. J Am Chem Soc. 2001; 123:8155–8156. [PubMed: 11506588]
12. Akinc A, Lynn DM, Anderson DG, Langer R. Parallel synthesis and biophysical characterization of a degradable polymer library for gene delivery. J Am Chem Soc. 2003; 125:5316–5323. [PubMed: 12720443]
13. Green JJ, Langer R, Anderson DG. A combinatorial polymer library approach yields insight into nonviral gene delivery. Acc Chem Res. 2008; 41:749–759. [PubMed: 18507402]
14. Anderson DG, Lynn DM, Langer R. Semi-automated synthesis and screening of a large library of degradable cationic polymers for gene delivery. Angewandte Chemie - International Edition. 2003; 42:3153–3158.
15. Vuorimaa E, Urtti A, Seppänen R, Lemmetyinen H, Yliperttula M. Time-resolved fluorescence spectroscopy reveals functional differences of cationic polymer-DNA complexes. J Am Chem Soc. 2008; 130:11695–11700. [PubMed: 18693688]
16. Olmsted J, Kearns DR. Mechanism of ethidium bromide fluorescence enhancement on binding to nucleic acids. Biochemistry (NY). 1977; 16:3647–3654.
17. Sarkar R, Pal SK. Interaction of hoechst 33258 and ethidium with histone1 - DNA condensates. Biomacromolecules. 2007; 8:3332–3339. [PubMed: 17902690]
18. Ketola T, Hanzlikova M, Urtti A, Lemmetyinen H, Yliperttula M, Vuorimaa E. Role of Polyplex Intermediate Species on Gene Transfer Efficiency: Polyethylenimine–DNA Complexes and Time-Resolved Fluorescence Spectroscopy. J Phys Chem B. 2011; 115:1895–1902. [PubMed: 21291220]
19. Yang J, Zhang P, Tang L, Sun P, Liu W, Sun P, et al. Temperature-tuned DNA condensation and gene transfection by PEI-g-(PMEO2MA-b-PHEMA) copolymer-based nonviral vectors. Biomaterials. 2010; 31:144–155. [PubMed: 19783298]
20. Kichler A, Leborgne C, Coeytaux E, Danos O. Polyethylenimine-mediated gene delivery: a mechanistic study. J Gene Med. 2001; 3:135–44. [PubMed: 11318112]
21. Akinc A, Thomas M, Klibanov AM, Langer R. Exploring polyethylenimine-mediated DNA transfection and the proton sponge hypothesis. J Gene Med. 2005; 7:657–663. [PubMed: 15543529]
22. Sonawane ND, Szoka FC Jr, Verkman AS. Chloride accumulation and swelling in endosomes enhances DNA transfer by polyamine-DNA polyplexes. J Biol Chem. 2003; 278:44826–44831. [PubMed: 12944394]
23. Xu Y, Szoka F Jr. Mechanism of DNA Release from Cationic Liposome/DNA Complexes Used in Cell Transfection. Biochemistry. 1996; 35:5616–5623. [PubMed: 8639519]
24. Sunshine J, Green JJ, Mahon KP, Yang F, Eltoukhy AA, Nguyen DN, Langer R, Anderson DG. Small-Molecule End-Groups of Linear Polymer Determine Cell-Type Gene-Delivery Efficacy. Adv Mater. 2009; 21:4947–4951.
25. Green JJ, Zugates GT, Tedford NC, Huang Y, Griffith LG, Lauffenburger DA, et al. Combinatorial modification of degradable polymers enables transfection of human cells comparable to adenovirus. Adv Mater. 2007; 19:2836–2842.
26. Zugates GT, Tedford NC, Zumbuehl A, Jhunjhunwala S, Kang CS, Griffith LG, et al. Gene delivery properties of end-modified poly(b-amino ester)s. Bioconjug Chem. 2007; 18:1887–1896. [PubMed: 17929884]

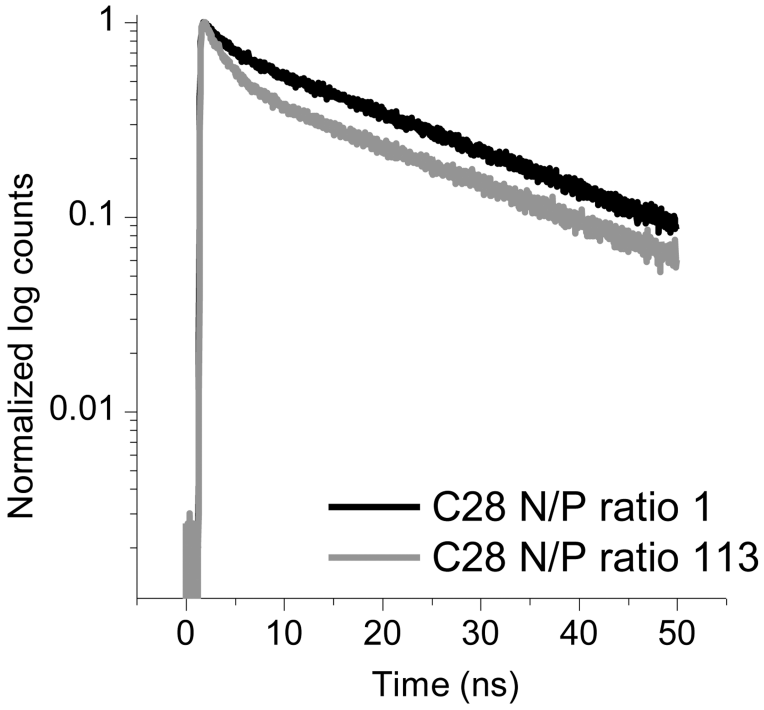

Fig. 1.
Normalized fluorescence decays at 610 nm for C28 with N/P ratio 1 and 113.

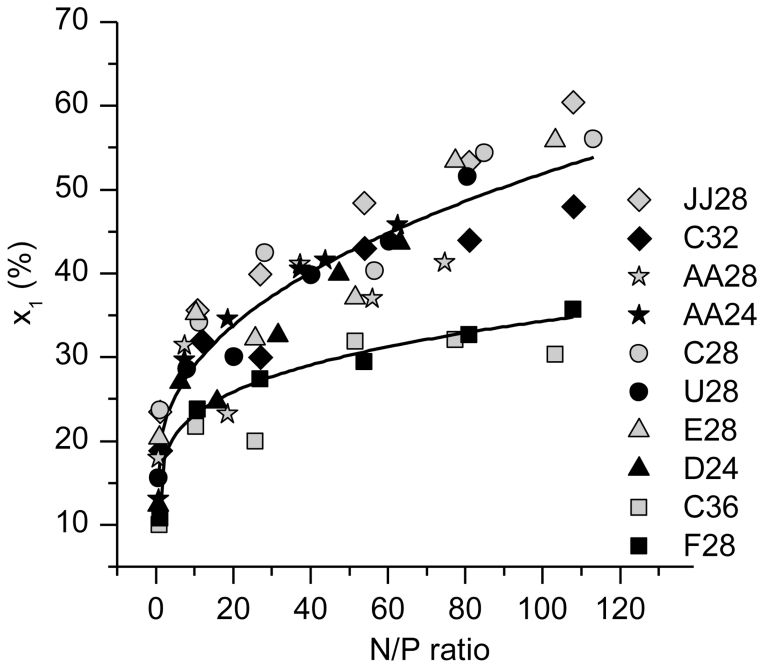

Fig. 2.
Proportion of the short-living decay component, x_1, as a function of N/P-ratio for the studied PBAEs.

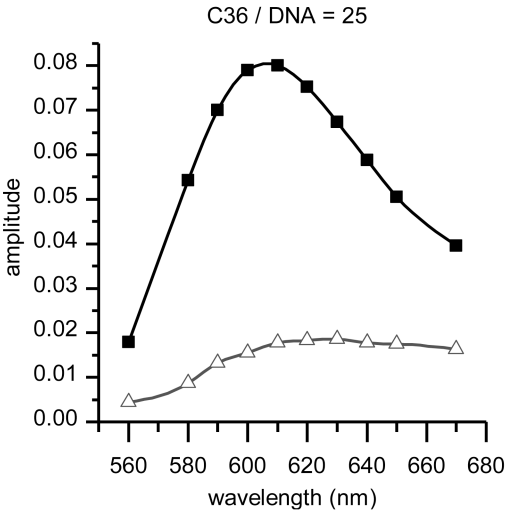

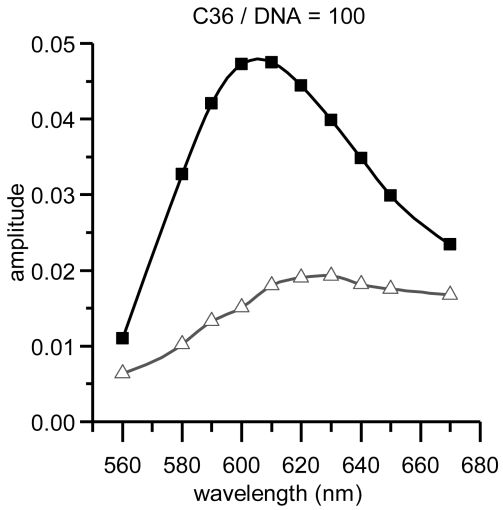

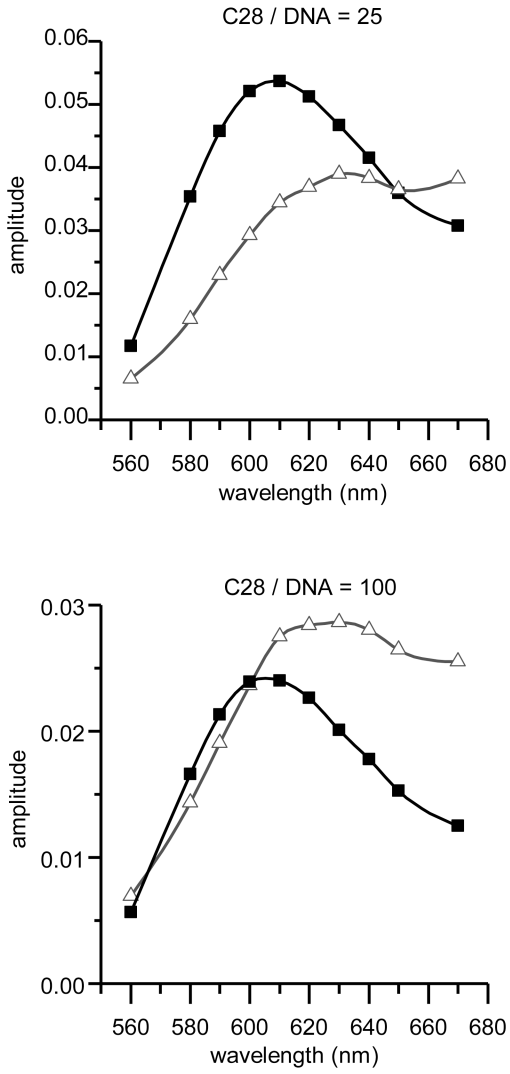

Fig. 3.

Decay associated spectra for C36 and C28 at N/P ratios 25 and 100. (Δ) short-living and (■) long-living decay component.

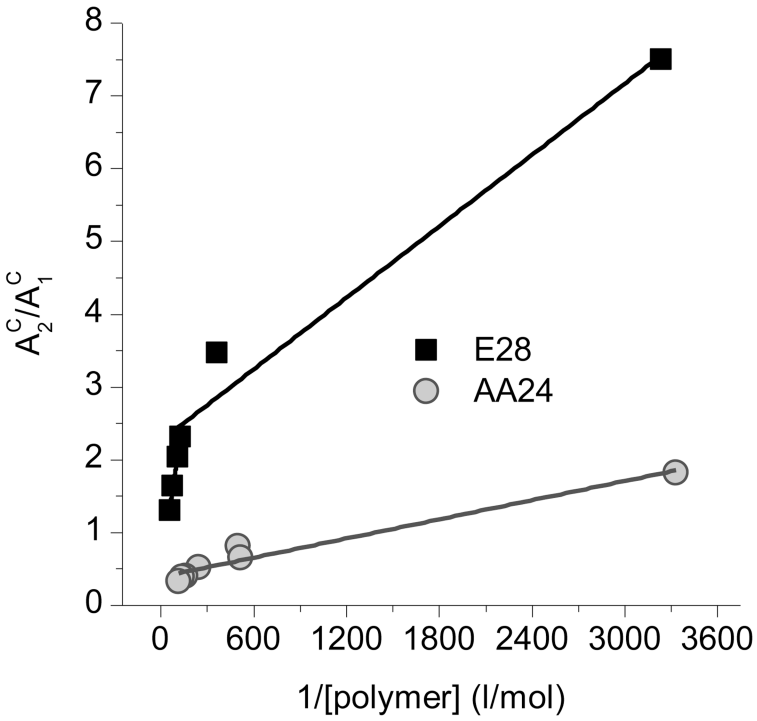

Fig. 4.

A_2^c/A_1^c as a function of 1/[polymer N-groups] for AA24 and E28.

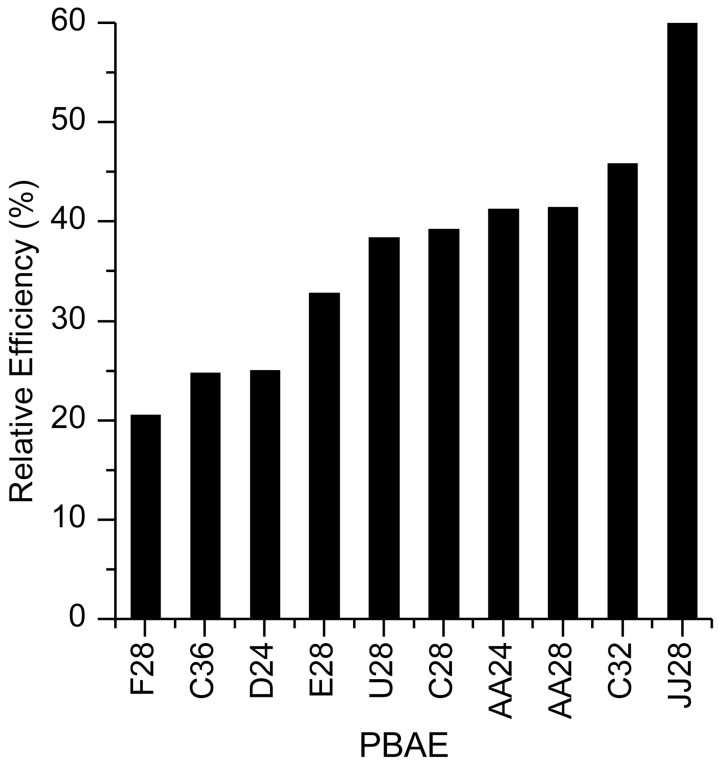

Fig. 5.
Relative efficiencies of the nanoparticle formation for the studied PBAEs determined by the fluorescence method. The relative error of the efficiencies is ±2%.

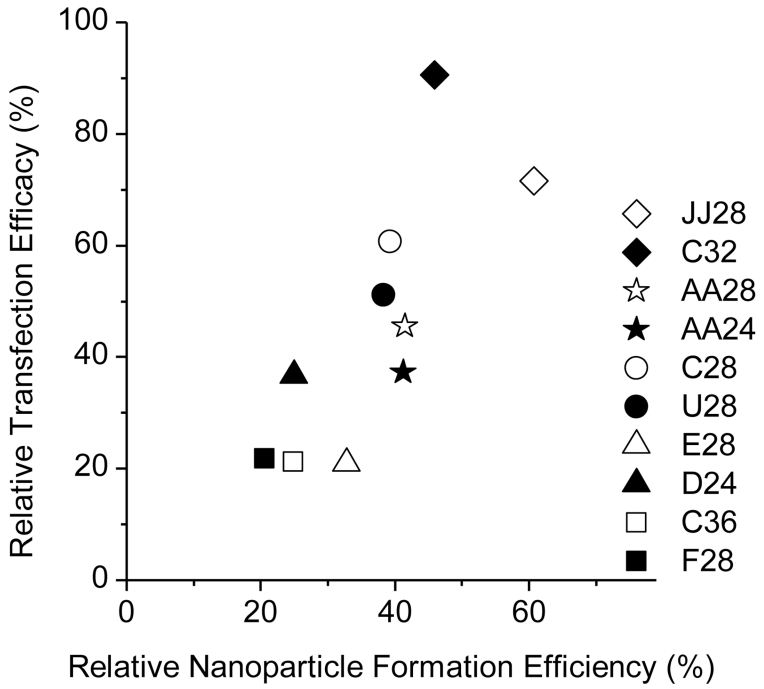

Fig. 6.
Correlation between the relative nanoparticle formation efficiency and the in vitro transfection efficacy.

Table 1

Structures of the diacrylate and amine monomers of the studied PBAEs, their average molecular weights (MW) and amine:acrylate ratios (Am:Ac).

Polymer MW (Da) Am/Ac	Diacrylate monomer	Amine monomer
F28 **16100** **1.025**	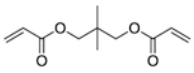	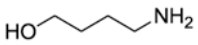
C36 21200 1.2	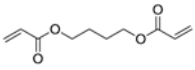	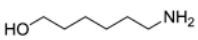
D24 9542 1.05	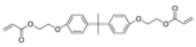	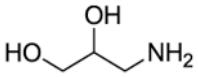
E28 14300 1.1	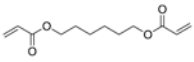	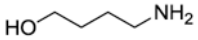
U28 15600 1.1	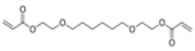	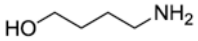
C28 27900 1.05	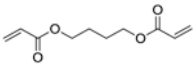	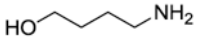
AA24 8058 1.3	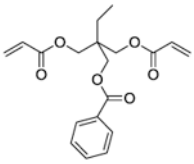	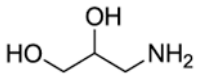
AA28 20900 1.1	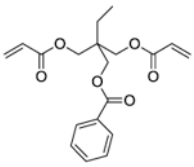	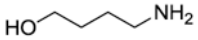
C32 18100 1.2	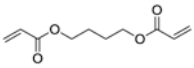	
JJ28 16800 1.1	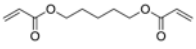	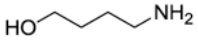
Synthesis of PBAEs	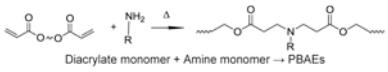	

Table 2

The average fluorescence lifetimes, $<\tau_i>$, for the studied PBAEs.

Polymer	$<\tau_1>$ (ns)	$<\tau_2>$ (ns)
F28	1.63 ± 0.16	22.53 ± 0.12
C36	1.75 ± 0.20	22.56 ± 0.14
D24	1.89 ± 0.16	22.35 ± 0.13
E28	1.75 ± 0.11	22.26 ± 0.14
U28	1.76 ± 0.13	22.32 ± 0.13
C28	1.84 ± 0.10	22.41 ± 0.15
AA24	1.79 ± 0.14	22.44 ± 0.14
AA28	1.73 ± 0.15	22.39 ± 0.14
C32	1.95 ± 0.12	23.18 ± 0.14
JJ28	1.86 ± 0.10	22.30 ± 0.15

Table 3

Molecular weights and binding constants determined as mol N-groups per dm^3 for the studied PBAEs. These binding constants were converted to the binding constants per molecule by $K_i' = (\text{average molecular weight of the polymer/molecular weight per N-group}) \times K_i$. The values for PEIs are from reference [18].

PBAE	M_{av} (kDa)	K_{tot} ($dm^3\ mol_N^{-1}$)[b]	K_{tot}' ($dm^3\ mol_{polymer}^{-1}$)[c]
F28	16.1	3870	2.1×10^5
C36	21.2	2090	1.4×10^5
D24	9.5	4020	7.5×10^4
E28	14.3	4550	2.1×10^5
U28	15.6	3950	1.5×10^5
C28	27.9	6220	6.0×10^5
AA24	8.1	2690	5.0×10^4
AA28	20.9	4700	2.3×10^5
C32	18.1	4440	2.7×10^5
JJ28	16.8	6100	3.4×10^5
linear PEI	22.0	6600	3.4×10^6
branched PEI	25.0	2100	1.2×10^6
branched PEI	0.7	4700	7.6×10^4

[a] dm^3 per mol N-groups

[b] dm^3 per mol polymer molecules